JOURNAL OF VIROLOGY, Jan. 1996, p. 468–477
0022-538X/96/$04.00+0

Vol. 70, No. 1

Extraction of Nuclei from Sonchus Yellow Net Rhabdovirus-Infected Plants Yields a Polymerase That Synthesizes Viral mRNAs and Polyadenylated Plus-Strand Leader RNA

JOHN D. O. WAGNER,† TAE-JIN CHOI,‡ AND ANDREW O. JACKSON*

Department of Plant Biology, University of California, Berkeley, California 94720

Received 16 June 1995/Accepted 16 October 1995

Although the primary sequence of the genome of the plant rhabdovirus sonchus yellow net virus (SYNV) has been determined, little is known about the composition of the viral polymerase or the mechanics of viral transcription and replication. In this paper, we report the partial isolation and characterization of an active SYNV polymerase from nuclei of SYNV-infected leaf tissue. A salt extraction procedure is shown to be an effective purification step for recovery of the polymerase from the nuclei. Full-length, polyadenylated SYNV N and M2 mRNAs and plus-strand leader RNA are among the products of the in vitro polymerase reactions. Polyadenylation of the plus-strand leader RNA in vitro is shown with RNase H and specific oligonucleotides. This is the first report of a polyadenylated plus-strand leader RNA for a minus-strand RNA virus, a feature that may reflect adaptation of SYNV to replication in the nucleus. Analysis of the SYNV proteins present in the polymerase extract suggests that the N, M2, and L proteins are components of the transcription complex. Overall, the system we developed promises to be useful for an in-depth characterization of the mechanics of SYNV RNA synthesis.

The rhabdoviruses comprise a large group of nonsegmented, negative-stranded RNA viruses. The best-characterized member of this group is vesicular stomatitis virus (VSV), which has served as a model system for the in vitro study of the RNA polymerases of the minus-strand viruses (for reviews, see references 3, 4, and 19). Even though in vitro viral polymerase activity has been reported for a number of rhabdoviruses other than VSV, in most cases this activity has not been characterized in detail (3). Therefore, little is known about the mechanics of the transcription and replication of other rhabdoviruses. Among those rhabdoviruses characterized at the level of primary RNA structure, the degree of sequence conservation is relatively low (8, 49). Moreover, individual members of this group infect a wide array of eukaryotic organisms. Thus, the viral polymerase complexes of other members of the family may differ from that of VSV in fundamental aspects that reflect their adaptation to different hosts.

Sonchus yellow net virus (SYNV) is the most extensively characterized among a group of more than 40 plant-infecting rhabdoviruses (for a review, see reference 31). The nucleus appears to be the site of SYNV replication as well as morphogenesis, a feature which SYNV shares with a number of plant-infecting rhabdoviruses, but not with any known animal rhabdoviruses (31). SYNV infection is associated with a pronounced swelling of the nuclei of infected cells (31), and nuclear inclusions have been observed in SYNV-infected cells (14). Virion maturation appears to occur through budding from the periphery of the nucleoplasm into the adjoining perinuclear space between the inner and outer nuclear membranes (59). Moreover, the presence of the viral nucleocapsid core in the nucleoplasm prior to budding has been demonstrated in SYNV-transfected cowpea protoplasts treated with tunicamycin, a glycosylation inhibitor (59).

The primary sequence of the 13,720-nucleotide (nt) minus-sense SYNV RNA genome has been determined in its entirety (see Fig. 1 and References 11, 12, 22, 26, 29, 55, and 63). The sequence indicates that the genome encodes at least six viral proteins, including a nucleocapsid protein (N), a putative phosphoprotein (M2), a putative matrix protein (M1), a glycoprotein (G), a putative core polymerase protein (L), and sc4, a viral protein of unknown function. SYNV gene expression occurs via transcription of the genomic RNA into discrete mRNAs that are polyadenylated in vivo (25, 33, 51). In addition to the six viral mRNAs, a small plus-strand leader RNA is also transcribed from the first 144 nt of the genomic RNA (62). Unlike several other minus-strand RNA viruses that replicate in the nucleus (40, 54), SYNV genes do not contain introns. Relatively little information is available concerning the mechanics of SYNV transcription (mRNA synthesis) and replication (genomic RNA synthesis). In particular, nothing is known about the primary polymerase products or the composition of the viral polymerase.

Although several groups have attempted to develop a protocol for recovery of in vitro SYNV transcriptase activity from purified virions (20, 30), the detection of high levels of RNA synthesis from the polymerase component of the virus particle has not been reported. As an alternative, we have investigated infected plant tissue fractions as a source of SYNV polymerase for in vitro study. In this paper, we describe a protocol for purification of tobacco leaf nuclei that are active in SYNV-specific RNA synthesis and a method for purification of the polymerase by salt extraction of the nuclei. The partially purified SYNV polymerase is able to transcribe SYNV mRNAs and polyadenylated plus-strand leader RNA. Leader RNA polyadenylation is a feature that distinguishes SYNV from other characterized nonsegmented, minus-stranded viruses (16, 41).

MATERIALS AND METHODS

Plants and virus. SYNV (ATCC PV-263) was maintained under ambient greenhouse conditions by serial passages in *Nicotiana edwardsonii*, a hybrid tobacco (13, 32). For purification of nuclei, leaf tissue showing the characteristic yellow netting was harvested between 10 and 14 days postinfection, at the onset

* Corresponding author. Phone: (510) 642-3906. Fax: (510) 642-9017.
† Present address: Division of Biology 147-75, California Institute of Technology, Pasadena, Calif.
‡ Present address: Department of Microbiology, National Fisheries of Pusan, Pusan, Korea.

of symptom development. The leaf tissue was frozen and stored at −80°C for up to 6 months. However, virus particles were purified from fresh leaf tissue by established procedures (32, 33).

Purification of nuclei. The protocol used for the isolation of nuclei was based on that of Schumacher et al. (56), with modifications. Frozen leaf tissue (80 to 100 g) was ground in liquid nitrogen, blended with 500 ml of nucleus isolation buffer (40% [vol/vol] glycerol, 600 mM sucrose, 25 mM Tris [pH 8.0], 5 mM $MgCl_2$, 2 mM spermine, 10 mM β-mercaptoethanol, 1 mM phenylmethanesulfonyl fluoride, and 1 mM benzamidine) in an Omnimixer (DuPont, Wilmington, Del.), and filtered through three successive layers of nylon mesh (350, 62, and 44 μm, respectively; Small Parts Inc., Miami, Fla.). Nonidet P-40 was added to 0.6%, and the slurry was stirred for 5 min. The nuclei were then pelleted by centrifugation for 10 min at 5,000 rpm in a Sorvall GSA rotor (DuPont; 3,000 × *g* average), resuspended in 3 to 5 ml of 95% (vol/vol) Percoll (Pharmacia, Piscataway, N.J.) in mannitol buffer (250 mM mannitol, 25 mM Tris [pH 8.0], 5 mM $MgCl_2$, 10 mM β-mercaptoethanol, 1 mM phenylmethanesulfonyl fluoride, and 1 mM benzamidine), and transferred to four 30-ml tubes. Each tube was brought to 15 ml with the 95% Percoll buffer, overlayered with 10 ml of mannitol buffer, and centrifuged for 10 min at 5,000 rpm in a Sorvall HB-4 rotor (3,000 × *g* average). The nuclei were then collected from the mannitol-Percoll interface of each tube, resuspended in 15 ml of mannitol buffer, and centrifuged as before onto a 10-ml 75% Percoll cushion (75% [vol/vol] Percoll in mannitol buffer). The nuclei from the interface and the upper half of the 75% Percoll cushion were washed in 15 ml of mannitol buffer, pelleted by centrifugation for 5 min at 2,500 rpm in the Sorvall HB-4 rotor (700 × *g* average), and then mixed with an equal amount of 2× extraction buffer [40% (vol/vol) glycerol, 200 mM $(NH_4)_2SO_4$, 25 mM hydroxyethylpiperazine ethanesulfonic acid (HEPES, pH 8.0), 5 mM $MgCl_2$, 3 mM dithiothreitol, 1 mM phenylmethanesulfonyl fluoride, 1 mM benzamidine, and 1 mM Pepstatin]. Either the preparations were frozen directly (purified nuclei), or the polymerase was extracted in the extraction buffer for 30 min at 4°C on a rocking mixer and then centrifuged for 30 min in an Eppendorf microcentrifuge at 14,000 rpm (10,000 × *g*, average) to clarify the supernatant. The resulting clarified supernatant (nuclear extract) was either used directly or frozen at −80°C.

In vitro reactions and RNA purification. In vitro polymerase reaction mixtures were incubated at 28°C in a total volume of 200 μl containing 20 μl of nuclei or nuclear extract in 6 mM $MgCl_2$–50 mM $(NH_4)_2SO_4$–12.5 mM HEPES (pH 8.0)–2 mM dithiothreitol–1 mM ATP–0.5 mM CTP–0.5 mM GTP–20 μM unlabeled UTP–50 μCi of [α-^{32}P]UTP–20 U of DNase I per ml–200 U of RNasin per ml (Promega, Madison, Wis.)–2% [vol/vol] glycerol, unless noted otherwise for specific experiments. Reactions were terminated by addition of sodium dodecyl sulfate (SDS) and EDTA to 0.5% and 10 mM, respectively, and the proteins were digested for 30 min at 42°C with proteinase K (20 μg/ml). RNA was purified by extraction in phenol-chloroform and precipitated twice in 750 mM ammonium acetate–70% ethanol, with 10 μg of *Saccharomyces cerevisiae* tRNA as a carrier.

Slot blot analysis. Slot blots were prepared by application of 5 μg of linearized, denatured double-stranded (ds) DNA to nitrocellulose with a manifold (Schleicher and Schuell, Keene, N.H.). RNA purified from in vitro reactions was hybridized to the blots for 48 h at 42°C in 30% formamide–300 mM NaCl–10 mM Tris (pH 7.4)–10 mM EDTA–0.2% SDS–200 μg of poly(A) RNA per ml. The blots were washed for 30 min at room temperature in 2× SSPE (360 mM NaCl, 20 mM Na_2HPO_4 [pH 7.6], 2 mM EDTA) containing 0.1% SDS, treated with RNase A (2 μg/ml in 2× SSPE) for 30 min at 37°C, and washed twice for 15 min at 67°C in 0.1 × SSPE–1% SDS. The radiolabeled RNA hybridized to the individual slots was quantified with a PhosphorImager (Molecular Dynamics, Sunnyvale, Calif.), and representative slots were counted in scintillation fluid. For quantification, purified RNA was hybridized in a dilution series to replicate slot blots. Typically, the radiolabeled RNA from both nuclei and nuclear extracts hybridized to each probe gave a linear response with respect to dilution, indicating that the DNA probe was saturating with respect to the viral RNA. Linear regression analysis was performed on each dilution series by using KaleidaGraph (Synergy Software, Reading, Pa.), and the slope of the best-fitting line for each probe was employed as a relative measure of specific hybridization.

Glyoxylation and agarose gel electrophoresis of RNA. Glyoxylation was carried out for 15 min at 55°C in reaction mixtures containing 3.75 μl of TES (10 mM Tris [pH 8.0], 1 mM EDTA, 0.2% SDS) containing various amounts of RNA, 0.25 μl of 1 M Na_2HPO_4 (pH 7.0), 21 μl of formamide, and 5 μl of glyoxyl. The glyoxylated RNA was electrophoresed through 1% agarose in TAE buffer (40 mM Tris-acetate, 1 mM EDTA) at 100 V until the bromophenol blue dye had migrated 8 cm. The gels were fixed overnight in 100% methanol and dried prior to analysis.

RNase H analysis. For RNase H analysis (36), the RNA samples were annealed to 1 μg of each oligonucleotide by heating to 90°C for 3 min in 50 mM Tris (pH 8.3)–10 mM dithiothreitol–60 mM NaCl (10-μl reaction mixtures), followed by slow cooling to 37°C. Magnesium chloride was added to 1.5 mM, and the RNA-DNA hybrids were digested with RNase H (0.5 U) for 30 min at 37°C. An equal volume of loading buffer (95% formamide, 0.25% bromophenol blue, 0.25% xylene cyanol FF) was added, the samples were denatured for 2 min at 85°C, and the RNA was resolved by polyacrylamide-urea gel electrophoresis.

Characterization of proteins. The antisera used included rabbit polyclonal antisera raised against disrupted SYNV virions (30) and mouse polyclonal ascites fluid specific to the SYNV L protein (SH1 2). To elicit the L-specific antibodies, a chimeric polypeptide consisting of the amino-terminal 198 amino acids of the L protein fused to glutathione *S*-transferase at the carboxyl terminus was used in Swiss Webster mice. An 8-amino-acid linker was present between the glutathione *S*-transferase and the L protein portion of the polypeptide. The antigen was obtained by protein overexpression in *Escherichia coli* transformed with the plasmid pGEXSH (see below). The overexpressed protein was extracted from cell lysates (15), purified by SDS-polyacrylamide gel electrophoresis (SDS-PAGE), and used to generate antibody-containing ascites fluid by established procedures (22).

SDS-PAGE was conducted on discontinuous gels (10% polyacrylamide in the separation gel, unless noted otherwise) as described previously (23). For Western blots (immunoblots), proteins were electrophoretically transferred to nitrocellulose (58). All incubations were in TBS (50 mM Tris [pH 7.4], 200 mM NaCl), containing 5% (wt/vol) nonfat dried milk and 0.1% (vol/vol) Tween 20. Crude extract from healthy *N. edwardsonii* leaves (75 μg of protein per ml) was added to primary antibody incubations to cross-absorb non-virus-specific components of the polyclonal antisera.

Plasmid constructs. A series of SYNV-specific clones (pJ3N1-pJ3L1 series, Fig. 1) containing ca. 800-nt fragments located at or near the 3′ end of each viral gene in the cloning vector pBSKS$^+$ II (Stratagene, La Jolla, Calif.) was constructed. In the SYNV genome (GenBank accession number L32603), pJ3N1 corresponds to positions 830 to 1633; pJ3T1 corresponds to 2011 to 2837; pJ3S1 corresponds to 3092 to 3863; pJ3O1 corresponds to 4308 to 5217; pJ3G1 corresponds to 6477 to 7155; and pJ3L1 corresponds to 12788 to 13630. For details of the construction of these plasmids, see reference 60. The 5′ and 3′ ends of each of these subclones were verified by sequence determination.

The plasmid pGEXSH, which was used for the production of the L-specific antiserum, contains a fusion of the glutathione *S*-transferase gene to nt 7184 to 7797 from the SYNV genome. This plasmid was generated by cloning a *Sma*I-*Hin*dIII fragment from the plasmid pGTFL2 (10) into the *Sma*I and *Eco*RI sites of the bacterial expression vector pGEX-2T (Promega).

Three additional clones used were pJW2, which corresponds to SYNV genome nt 1 to 265; p3ZT1 (nt 1750 to 2837); and p3ZN1 (nt 203 to 1627). The SYNV-specific insert in pJW2 was obtained by PCR from the plasmid pGS2 (62). The DNA fragment resulting from PCR was digested with *Eco*RI-*Hin*cII and cloned into the corresponding sites in the vector pBSKS$^+$ II. The plasmid p3ZT1 was constructed in pGEM3Z at the *Eco*RI and *Pst*I sites. The insert contains two fragments, an *Eco*RI-*Nco*I fragment containing the tobacco etch virus 5′ nontranslated leader from pRTL2-gus (50) and an *Nco*I-*Pst*I fragment containing the entire open reading frame of the M2 gene, derived from the plasmids pGL57 (26) and pAS35 (26), as described in reference 60. The plasmid p3ZN1 is similar to p3ZT1, except that it contains two fragments in place of the M2 gene: an *Nco*I-*Bam*HI fragment containing the entire N gene open reading frame (obtained by PCR amplification of the fragment from pNS3 [60]) and a *Bam*HI-*Eco*RV fragment containing the bacteriophage T7 termination sequence from pET3C (57), which are cloned sequentially between the *Nco*I site at the 3′ end of the tobacco etch virus 5′ nontranslated leader and the *Hin*dIII site in the vector (filled in). Sequence determination of the SYNV-derived inserts in pJW2 and p3ZN1 revealed that pJW2 is identical to the published sequence in the corresponding region, whereas p3ZN1 contains two modifications, including a 3-nt insertion between the 5′ ATG and the second codon, designed to generate an *Nco*I site (which encodes an alanine not present in the viral gene), and a single-nucleotide insertion following nt 1418, which presumably arose during PCR amplification. For the purpose of the experiments presented here, these modifications are unimportant.

Data presentation. Gel electrophoresis results were obtained by PhosphorImager exposures and were passed through Adobe Photoshop (Adobe Systems, Mountain View, Calif.) for presentation. Aside from the alteration of the order of the lanes, the data were not modified.

RESULTS

Characterization of RNA synthesis in purified nuclei. Because the plant cell nucleus appears to be the site of SYNV transcription and replication, we initiated attempts to purify and characterize a virus-specific polymerase by purifying nuclei from infected tobacco leaves. The nuclei were purified with Percoll gradients in a modified version of the protocol developed by Schumacher et al. (56). The resulting preparations were gray or light green and contained intact nuclei as well as some nuclear fragments, as judged by light microscopy. Purified nuclei were tested in vitro for the ability to synthesize plus- or minus-strand SYNV RNA. RNA from nuclei incubated in the presence of [α-^{32}P]UTP was purified and hybridized to unlabeled double-stranded DNA probes (Fig. 1) immobilized on nitrocellulose filters. As shown in Fig. 2, the production of SYNV-specific RNA in vitro was easily detectable in nuclei from infected leaf tissue, in sharp contrast to nuclei isolated

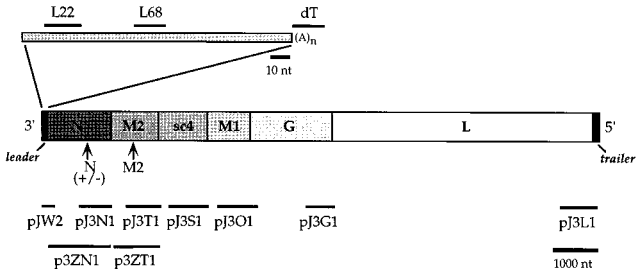

FIG. 1. Scale drawing of the SYNV genome showing the location of the probes used for slot blot and RNase H analyses. The genomic locations and relative sizes of the viral genes are illustrated, as well as the plus-strand leader and trailer. The genomic location of a series of cDNA probes (thick bars) used in slot blot hybridizations is shown below the genome. In addition, the arrows show the locations of the N and M2 mRNA-specific DNA oligonucleotides. In the SYNV genome (GenBank accession number L32603), these oligonucleotides are located at positions 1068 to 1049 and 2297 to 2281, respectively. A third oligonucleotide that is complementary to the same position on the genomic RNA as the N mRNA-specific oligonucleotide was also used as a control. The plus-strand leader RNA is shown above the genome, with the locations and sizes of oligonucleotides used for hybridization illustrated to scale. The plus-strand leader-specific oligonucleotides correspond to nt 76 to 60 (L68) and 31 to 12 (L22) in the SYNV genome. Also shown is the site of oligo(dT) hybridization to the leader RNA, as suggested by the analysis presented in Fig. 6. The scale bar below the genome represents 1,000 nt, and the bar below the plus-strand leader represents 10 nt.

from mock-infected tissue. The radioactivity binding to the SYNV M2-specific probe in reactions with the infected nuclei was approximately 1,000-fold greater than that of uninfected nuclei (Table 1). In similar experiments, labeled RNA hybridized to probes derived from regions of each of the six viral genes, indicating that viral transcription and/or replication occurred in vitro along the length of the genome (data not shown). As expected, endogenous host RNA polymerase activity was also detected in the purified nuclei. The amount of radiolabeled RNA that hybridized to a probe with genes coding for rRNA derived from pea exceeded that hybridized to an SYNV-specific probe in the infected nuclei (compare rRNA with M2 in Fig. 2) and was over 200-fold above background in the uninfected nuclei (Table 1). Because of high levels of nonviral transcription activity, as well as apparent RNase activity in the nuclei (data not shown), the viral RNA synthesized in the purified nuclei was not characterized further.

Extraction of SYNV polymerase activity from nuclei. Salt extraction of the purified nuclei was investigated as a means to purify viral polymerase activity. Extraction of purified nuclei has been employed extensively for partial purification of a variety of enzymatically active complexes from the nucleoplasm, including eukaryotic RNA polymerases, pre-mRNA splicing machinery, and mRNA polyadenylation activity (17, 27, 37, 46). Because the choice and concentration of monovalent salt in various extraction procedures have been shown to be critical for subsequent enzymatic activity (27, 43), several salts including $(NH_4)_2SO_4$, KCl, potassium glutamate, and NaCl were tested at concentrations ranging from 50 to 800 mM. Extraction in 50 to 100 mM $(NH_4)_2SO_4$ released the highest levels of SYNV polymerase activity into the nuclear extract (data not shown). The optimal concentration of the other monovalent cations varied considerably. Setting the amount of SYNV RNA synthesis detected in extracts prepared in 100 mM $(NH_4)_2SO_4$ as 100%, the maximal activities detected with the other salts were 95% in 800 mM KCl, 80% in 400 mM NaCl, and <20% in 800 mM potassium glutamate (results are the average of four determinations from two independent extraction series).

High levels of SYNV RNA synthesis in vitro were detected after extraction of the nuclei with optimal concentrations of $(NH_4)_2SO_4$. The amount of RNA products synthesized in extracts derived from infected versus control leaves that hybridized to the SYNV M2 probe differed by 3 orders of magnitude (Fig. 2, nuclear extract panels, and Table 1). Furthermore, the amounts of genes coding for rRNA and negative control probe hybridization were nearly the same with radiolabeled RNA from the extracts (Fig. 2; Table 1). This suggests that only small amounts of RNA polymerase I activity present in the nuclei were recovered in the 100 mM $(NH_4)_2SO_4$ nuclear extracts. Thus, with endogenous rRNA synthesis as a reference, it appears that the virus-specific polymerase was largely responsible for RNA synthesis in the extracts from infected leaf nuclei. In addition, the amounts of protein in the nuclei and the same volume of polymerase extract were measured and used to calculate the specific activity of the SYNV polymerase in each preparation (defined as counts per minute incorporated into SYNV RNA per microgram of total protein, with the RNA hybridized to an arbitrary SYNV probe in the slot blot assay as a measure). Salt extraction resulted in at least a 20-fold concentration of the specific activity of the polymerase (Table 1). Therefore, these results demonstrated that the ammonium sulfate extraction procedure was an effective means for purifying SYNV intracellular polymerase activity from nuclei of infected *N. edwardsonii* tissue. For convenience, the terms polymerase extract and control extract will be used henceforth to identify the nuclear extracts from SYNV-infected tissue and those from mock-infected tissue, respectively.

SYNV RNA transcription is the primary activity in the polymerase extracts. SYNV RNAs present in infected tissue and protoplasts have discrete sizes that correspond to the six viral genes (the viral mRNAs) and the full-length viral RNA (25). To investigate whether similar RNAs were synthesized in vitro in polymerase extracts, we developed a protocol to score for the size distribution of the radiolabeled RNA corresponding to each of the six viral genes. The RNA synthesized in a 1-h reaction was purified, denatured by glyoxylation, and electrophoresed through low-melting-point agarose. The agarose was then cut into longitudinal slices, and the radiolabeled RNA in each slice was quantified following hybridization to replicate slot blots containing cDNA probes from the 3′ end of each of the six viral genes (for probe location, see Fig. 1). Using this procedure, we can distinguish between viral transcription and replication, on the basis of the size of the products. Furthermore, the relative levels of transcription of individual SYNV genes can be compared.

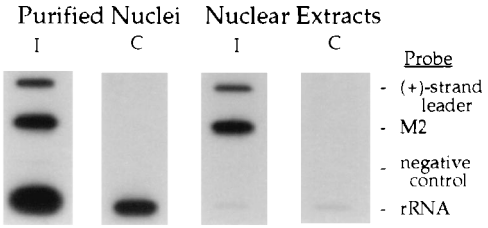

FIG. 2. Slot blot analysis of RNA synthesis in purified tobacco leaf nuclei and in nuclear extracts. Nuclei and nuclear extracts were prepared from SYNV-infected (I) and control (C) tobacco leaf tissue. Radiolabeled RNA synthesized in vitro by each preparation was purified and hybridized to replicate slot blots containing linearized DNA plasmid probes corresponding to the plus-strand leader and the first 100 nt of the N gene (pJW2), the M2 gene (p3ZT1), a negative control (the plasmid vector pBSKS$^+$ II), and rRNA (pRS1). In this experiment, 200-μl reaction mixtures containing 50 μl of nuclei or nuclear extracts and 35 μCi of [α-^{32}P]UTP were incubated for 30 min under otherwise standard conditions.

TABLE 1. Quantitative analysis of RNA synthesis in purified tobacco leaf nuclei and in nuclear extracts[a]

Sample	Type	SYNV probe		Negative control (cpm)	rRNA (cpm)	M2/rRNA ratio	Protein concn[b] (mg/ml)	Sp act (cpm/μg)
		1-N (cpm)	M2 (cpm)					
Nuclei	Infected	600	2.5×10^3	55	1.4×10^4	0.2	9.0	5.6
	Mock	23	12	23	1.2×10^3			
Nuclear extracts	Infected	440	1.9×10^3	13	50	37	0.4	93.0
	Mock	9.6	2.1	3	33			

[a] Quantification of the data presented in Fig. 2.
[b] Determined by the Bradford assay (7) as follows. Nuclei and nuclear extracts (100 μl) were diluted in 900 μl of Tris-EDTA and sonicated four times for 20 s. Each sample was cooled on ice for 40 s between sonications. The samples were then centrifuged for 5 min at 10,000 × *g* in a microcentrifuge, and the protein content of the supernatant was determined. The values represent the average of four independent determinations of each sample.

To provide size markers for the SYNV RNAs and to test the efficacy of the separation-hybridization system, four radiolabeled RNAs of known size were prepared from linearized plasmid DNA with the bacteriophage polymerase T7 or SP6. This RNA was added to the RNA synthesized in the polymerase extract prior to glyoxylation. The cDNA corresponding to each RNA was included on the slot blots. As shown in Fig. 3A, the four marker RNAs were effectively separated and could be localized to specific gel slices.

On the basis of comparison of the size of each SYNV mRNA with the size of the RNA markers, full-length N (1,551 nt), M2 (1,138 nt), sc4 (1,196 nt), and M1 (1,071 nt) transcripts should fractionate into slice 5, full-length G (2,045 nt) should fractionate into slice 5 or 4, and full-length L (6,400 nt) should fractionate into slice 4. In contrast, full-length 13,720-nt genomic or antigenomic RNAs should fractionate into slice 3. The greatest quantity of radiolabeled RNA hybridized to the N gene probe (Fig. 3B). Most of this RNA was located in slice 5, suggesting that full-length viral N mRNA was produced in vitro. In addition, a considerable amount of the M2, sc4, and M1 transcripts were also found in slice 5 (Fig. 3C). However, a significant proportion of the RNAs that hybridized to the M2, sc4, and particularly the M1 probes were shorter than the native mRNAs and were located in the fractions containing smaller RNAs. These transcripts could have been nascent RNA intermediates or RNA degradation products, or they might have arisen from premature termination of mRNA synthesis. Importantly, a precipitous drop in transcript abundance between gel slices 5 and 4 was detected with probes to each of these four genes, suggesting that specific termination or cleavage of discrete RNA transcripts occurred during the in vitro synthesis reaction. Full-length G and L mRNAs (2,044 and 6,400 nt, respectively) were not detected (Fig. 3D). Thus, if these mRNAs were produced in vitro, their abundance was significantly lower than those of the shorter RNA species that hybridized to the G and L probes. Little or no appreciable RNA hybridization was detected with any probe in gel slice 3, suggesting that full-length viral replication was not responsible for the RNA synthesis detected. Overall, after 1 h, the products detected corresponded in size to full-length or less viral mRNAs, suggesting that viral transcription, rather than replication, was the primary activity. Furthermore, the transcript size heterogeneity increased, while full-length product accumulation decreased, corresponding to the location relative to the 3′ end of the genome of each putative mRNA. These results are consistent with a cascade pattern in the rate of mRNA accumulation which reflects the location of each gene on the viral genome, from 3′ to 5′.

In addition to the slot blot assay, the products of 1-h in vitro reactions were analyzed directly by agarose gel electrophoresis under denaturing conditions. The RNA produced in 1 h in the polymerase extract from SYNV-infected tissue contained a prominent band of approximately 1,500 nt, as well as heterogeneous RNAs of approximately 1,000 nt (Fig. 4, lane 3). In contrast, in the control extract (Fig. 4, lane 4), essentially no discrete, de novo-synthesized RNA species were evident. This result confirms the analysis presented in Fig. 2 and Table 1, indicating that little host polymerase activity was present in the nuclear extracts. Formally, the RNAs detected could have been radiolabeled by UTP incorporation during RNA chain elongation or, alternatively, by modification of preexisting RNA involving the transfer of the labeled α-phosphate group. As a control, therefore, GTP methylated at the 3′ hydroxyl group was substituted for unmethylated GTP in the reaction. This substitution resulted in virtual elimination of RNA radiolabeling (Fig. 4, lane 5). Thus, GTP with an available 3′ hydroxyl group was required for incorporation of the α-phosphate of UTP into RNA, as would be expected for an RNA elongation reaction, but not alternative reactions involving preexisting RNA. One distinguishing feature of the products of minus-strand virus replication is that they are encapsidated by the viral nucleocapsid protein and are therefore resistant to micrococcal nuclease, unlike the viral transcription products (9, 28). As shown in Fig. 4, lane 6, treatment with micrococcal nuclease (10 μg/ml) after in vitro RNA synthesis in the polymerase extract, but prior to RNA extraction, led to the almost total degradation of the radiolabeled RNA. Encapsidated VSV and measles viral RNA was resistant to the 10-μg/ml nuclease concentration used (9, 28). Thus, it is unlikely that the de novo-synthesized RNA was encapsidated; this result suggests that SYNV transcription exceeds replication in the system, in agreement with the results presented in Fig. 3.

Identification of polyadenylated N and M2 mRNA in vitro transcription products. The data presented in Fig. 3 suggested that full-length mRNAs for several of the viral genes, including the N, M2, sc4, and M1 genes, might be synthesized in vitro. Furthermore, the mobility in agarose gels of RNA markers transcribed in vitro by T7 polymerase from full-length cDNA clones of the SYNV N and M2 genes (Fig. 4, lanes 1 and 2), was similar to that of the two major clusters of RNA products synthesized in the polymerase extracts (Fig. 4, lane 3). Therefore, using RNase H analysis, we next sought to unambiguously identify the SYNV N and M2 mRNAs as components of the reaction products. RNase H specifically degrades RNA in RNA-DNA heteroduplexes, so that RNA digestion in the presence of a chosen DNA oligonucleotide is diagnostic for the presence and location of a specific sequence in a given RNA molecule. Radiolabeled RNA synthesized in 1-h in vitro reactions containing the polymerase extract was hybridized to a DNA oligonucleotide complementary to nt 902 to 921 of the SYNV N mRNA, a complementary oligonucleotide (genomic sense specific), or an oligonucleotide complementary to nt 581

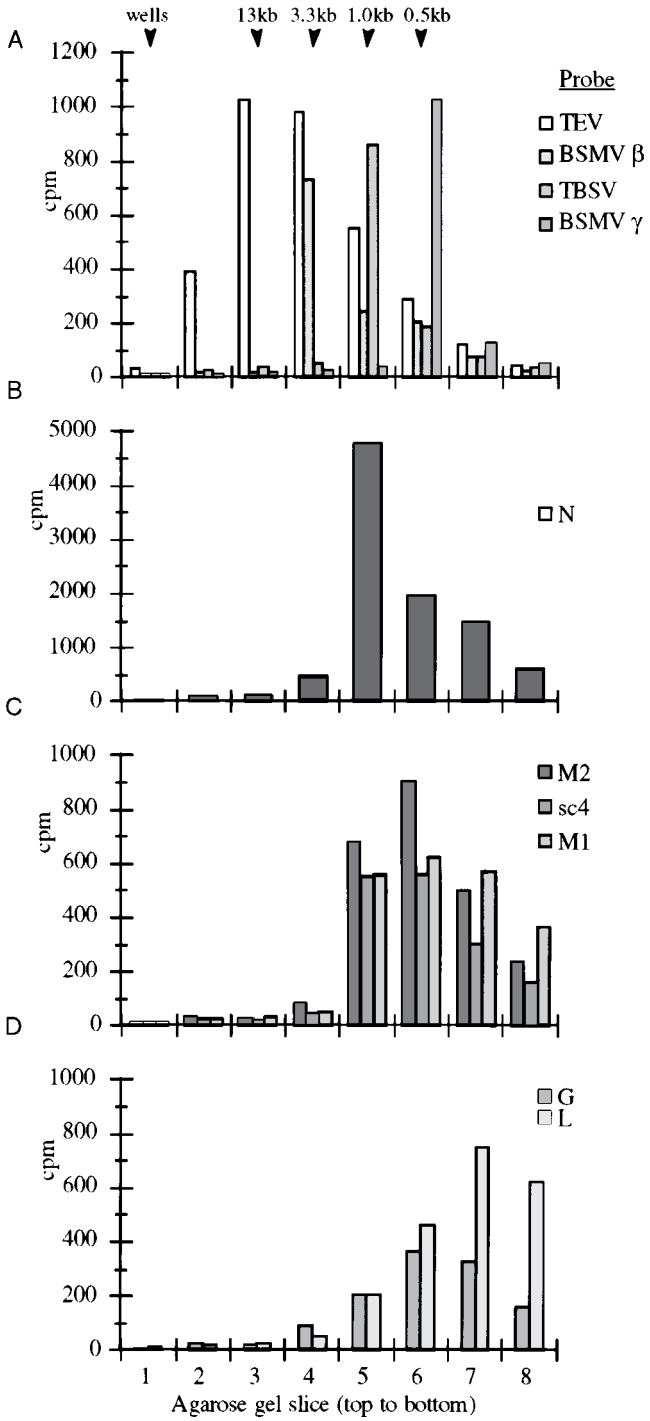

FIG. 3. Analysis of the size distribution of SYNV RNAs synthesized during a 1-h incubation of the polymerase extract. RNA radiolabeled in vitro was fractionated on an agarose gel, and the size distribution of specific RNAs was determined by slot blot hybridization of the fractions. Radioactivity hybridized to double-stranded DNA probes for specific RNAs is depicted in counts per minute. (A) Internal RNA size markers; (B) the SYNV N gene; (C) the SYNV M2, sc4, and M1 genes; (D) the SYNV G and L genes. The SYNV probes correspond to the pJ3N1-pJ3L1 series that is illustrated in Fig. 1. The location of each RNA size marker is shown with an arrowhead above the appropriate gel slice. RNA markers were produced from linearized plasmids with T7 or SP6 RNA polymerases. Plasmids used for the marker synthesis and on the slot blot were as follows: 13 kb, pTEV7D-GUS.P1 (18), linearized with *Bgl*II; 3.3 kb, β 42Sp1 (48), linearized with *Bgl*II; 1.0 kb, pTBSV-100 (24), linearized with *Stu*I; 0.5 kb, γ 42 (48), linearized with *Eco*RV. For this experiment, the RNA radiolabeled in a 200-μl reaction (with 100 μl of polymerase extract and 500 μCi of [α-^{32}P]UTP) was purified, glyoxylated, and separated on a 1% low-melting-point agarose gel. Prior to hybridization, the gel was soaked in 50 mM sodium hydroxide for 15 min to partially degrade the RNA and then neutralized by soaking in 300 mM sodium acetate (pH 5.8) for a further 15 min. The gel was cut into eight 1-cm longitudinal slices, and the RNA was released and denatured by heating at 100°C for 3 min. Each sample was brought to 10 ml in hybridization buffer, and the RNA was hybridized to slot blots.

to 597 of the M2 mRNA (see Fig. 1 for location), and the samples were digested with RNase H. The RNA products were then denatured and separated by agarose gel electrophoresis (Fig. 5, lanes 1 to 4). Note that these RNAs were poly(A) selected with oligo(dT) cellulose prior to the RNase H analysis to increase the clarity of the results (see below). Figure 5, lane 1, shows that, in the presence of the oligonucleotide complementary to the N mRNA, the ca.-1,500-nt RNA product of the polymerase extract reaction was cleaved into two discrete bands of lower molecular weight. Similarly, after hybridization of the RNA to the M2-specific oligonucleotide, the band of the predicted size for the M2 RNA was largely cleaved by RNase H into smaller products (Fig. 5, lane 2). In contrast, cleavage was not observed in the presence of the genomic sense-specific oligonucleotide or in reaction mixtures lacking an oligonucleotide (Fig. 5, lanes 3 and 4, respectively).

In parallel controls, a mixture of N and M2 RNAs transcribed by T7 polymerase from the full-length clones was digested with RNase H following hybridization to the DNA oligonucleotides (Fig. 5, lanes 5 to 8). An oligonucleotide-specific cleavage pattern was also observed with these RNAs, providing strong evidence for the specificity of the cleavage reaction. Furthermore, since the sequence of the DNA plasmids used for T7 transcription is known, the size of the RNA cleavage products (shown to the left in Fig. 5) can be used as a measure for cleavage products from the polymerase reaction. Cleavage of full-length N mRNA is expected to yield a 5′ end cleavage product of 901 nt and a 3′ end product of 629 nt and additional poly(A) tail; full-length M2 mRNA is expected to yield products of 580 nt (5′ end) and 541 nt, plus poly(A) tail (3′ end). Comparison of the cleavage products of N and M2 RNAs synthesized with polymerase extract and T7 polymerase reveals that the polymerase extract products were appropriately sized for products derived from SYNV N and M2 mRNAs (Fig. 5, compare lanes 1 and 5 and lanes 2 and 6). In sum, these experiments provided compelling evidence that two predominant RNA products synthesized in 1-h in vitro reactions containing the polymerase extract corresponded in size and sequence to full-length SYNV mRNAs.

SYNV mRNAs synthesized in vivo are polyadenylated at the 3′ end and thus bind selectively to oligo(dT)-cellulose (25). The RNAs synthesized in a 1-h in vitro reaction in the polymerase extract were therefore also examined by passage over oligo(dT)-cellulose columns. Electrophoretic separation of the RNA selected by binding to oligo(dT) (Fig. 5, lane 9) revealed that this RNA is clustered in two bands, which, on the basis of the RNase H analysis, contain at least the N and M2 mRNAs. Although a specific assay was not conducted, the lower band may also contain the sc4 and M1 mRNAs. In contrast, the RNA that did not bind the oligo(dT) (Fig. 5, lane 10) exhibited greater size heterogeneity but was principally found in two broad clusters that were shorter in length than the SYNV N or the M2-sc4-M1 mRNAs. A simple interpretation of these results is that the full-length viral mRNAs were polyadenylated and were therefore oligo(dT) selected, while smaller transcription intermediates or degradation products lacked the poly(A) sequences.

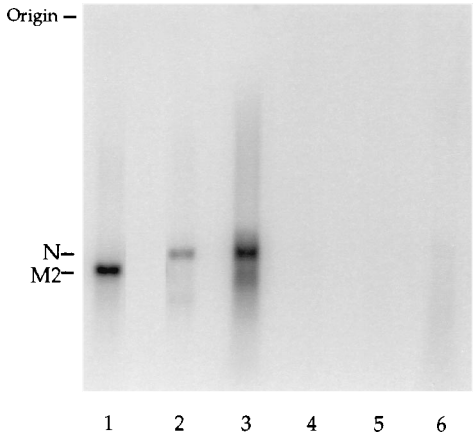

FIG. 4. Agarose gel analysis of RNAs synthesized by polymerase and control extracts in vitro. RNA synthesized after 1 h in vitro was purified, glyoxylated, and electrophoresed through a 1% agarose gel. Lanes 1 and 2 contain RNA synthesized by T7 polymerase from a full-length cDNA clone of the M2 gene (p3ZT1) and the N gene (p3ZN1), respectively. Lanes 3 and 4 show RNA products synthesized by the SYNV polymerase extract or the control extract from uninoculated plants, respectively. Lane 5 was loaded with products of a reaction with the polymerase extract under standard conditions except for substitution of 3′-O-methylated GTP (0.5 mM) for GTP. Lane 6 shows digestion of the RNA products synthesized in the polymerase extract following micrococcal nuclease (10 μg/ml [9]) prior to phenol extraction. The migration of these RNAs is shown on the left.

As a control, radiolabeled RNA synthesized in vitro by T7 bacteriophage polymerase transcription of full-length N and M2 cDNA clones was also fractionated on oligo(dT)-cellulose columns. Fortuitously, these two full-length cDNA clones differ in that the M2 cDNA contains a ca.-15-nt adenylate tail following the genome-encoded sequence that was retained during cDNA cloning, whereas the N cDNA terminates at the 3′ end of the genome-encoded open reading frame. Comparison of the oligo(dT)-bound fraction (Fig. 5, lane 11) and the flowthrough fraction (Fig. 5, lane 12) reveals that the oligo(dT)-cellulose effectively bound the T7 polymerase-synthesized polyadenylated M2 RNA but not the nonpolyadenylated N RNA. Thus, this important control experiment demonstrates that the retention by oligo(dT) of the N mRNA synthesized in the SYNV polymerase extract must be due to sequences [most likely a 3′ end-terminal poly(A) extension] that are not present in the T7-synthesized RNA.

The concentration of both the monovalent and divalent cations was likely to be a critical factor in polymerase activity in vitro. Therefore, the effect of $(NH_4)_2SO_4$ and $MgCl_2$ concentration on RNA synthesis in polymerase extracts was examined. The results of experiments (not shown; 1-h reactions) revealed that maximal levels of N mRNA were synthesized in 6 mM $MgCl_2$ (from a range of 0.5 to 12 mM) and 50 mM $(NH_4)_2SO_4$ (from a range of 10 to 100 mM). Inspection of the RNA products following gel electrophoresis indicated that the relative size profiles of the products were similar under all conditions (except at very low concentrations of $MgCl_2$), suggesting that the ion concentration primarily influences the rate rather than the processivity of the transcriptase (data not shown). The salt optima for SYNV transcription did not differ significantly from those determined previously for VSV transcription in vitro (2).

SYNV plus-strand leader is synthesized and polyadenylated in vitro. A positive-strand leader RNA of 144 to 145 nt that is complementary to the 3′ end of the SYNV genome is present in SYNV-infected cells and protoplasts (12, 62). This leader RNA binds to oligo(dT)-cellulose, which may be suggestive of polyadenylation at the 3′ end. To examine the products of the in vitro reactions for the presence of plus-strand leader RNAs, and to characterize these molecules, we used the oligonucleotides depicted in the upper portion of Fig. 1 in RNase H analyses. The results revealed that both synthesis and polyadenylation of plus-strand leader RNA occurred during the 30-min in vitro reactions (Fig. 6). In control experiments, RNA products that bound to oligo(dT)-cellulose [poly(A)$^+$ fraction], either without further treatment (not shown) or after RNase H digestion in the absence of an oligonucleotide (Fig. 6A, lane 1), formed a smear of RNA of approximately 150 to 250 nt on an 8% polyacrylamide gel. RNase H digestion in the presence of oligo(dT) converted the heterogeneous RNA into a broad band of slightly less than 147 nt, indicating the presence of a poly(A) extension on the uncleaved RNA (Fig. 6A, lane 2). Cleavage of the heterogeneous 150- to 250-nt RNAs in the presence of L68, an oligonucleotide complementary to bases 60 to 76 of the leader RNA, demonstrated that these molecules corresponded to plus-strand leader RNAs (Fig. 6A, lane 3). The products of this cleavage reaction included a cluster of five bands between the 57- and 67-nt markers (cluster II), as well as an RNA ladder of approximately 70 to 190 nt in length (cluster I). Addition of oligo(dT) to the cleavage reaction with L68 had no effect on the products in cluster II, while those in cluster I were converted into a ladder of ca. 70 to 75 nt (Fig. 6A, lane 4), suggesting that the products in cluster I, but not those in cluster II, were polyadenylated. Digestion with L68 together with L22, an oligonucleotide complementary to bases 1 to 30 of the leader RNA, produced a series of bands ranging in size from 26 to ca. 35 nt, but the bands in cluster II were absent (Fig. 6A, compare lane 5 with lane 3). In contrast, no effect on the cluster I products was

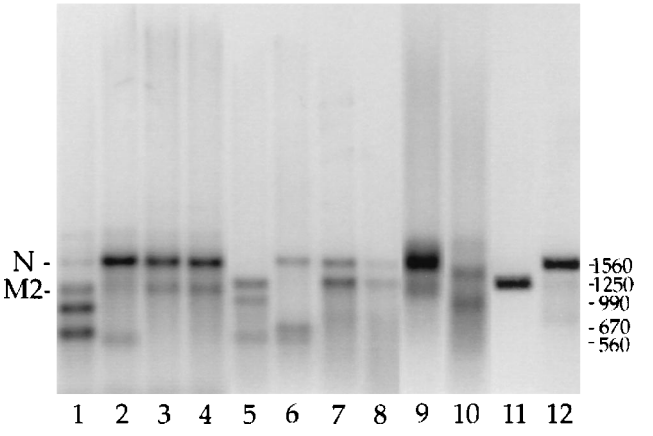

FIG. 5. An agarose gel showing results of RNase H analysis and oligo(dT)-cellulose fractionation of RNA synthesized by polymerase extracts in vitro. RNase H analysis was conducted with poly(A)-selected RNAs synthesized by the polymerase extract (two 200-μl reaction mixtures, pooled, lanes 1 to 4) or by T7 polymerase from the N and M2 cDNA clones (lanes 5 to 8). Aliquots of each RNA preparation were digested with RNase H after hybridization to the mRNA sense-specific N oligonucleotide (lanes 1 and 5), the mRNA sense-specific M2 oligonucleotide (lanes 2 and 6), or the genomic sense-specific N oligonucleotide (lanes 3 and 7) or hybridization in the absence of added oligonucleotide (lanes 4 and 8). In a separate experiment, RNA synthesized in vitro by the polymerase extract in two 200-μl reaction mixtures (pooled, lanes 9 and 10) or by T7 polymerase from full-length cDNA clones of the N (p3ZN1) and M2 (p3ZT1) genes (also pooled, lanes 11 and 12) was fractionated by oligo(dT)-cellulose. Lanes 9 and 11 show the RNAs bound by oligo(dT)-cellulose, and lanes 10 and 12 contain the unbound fractions. The predicted sizes of the T7 RNAs in nucleotides are shown on the right; the migration of these RNAs is shown on the left.

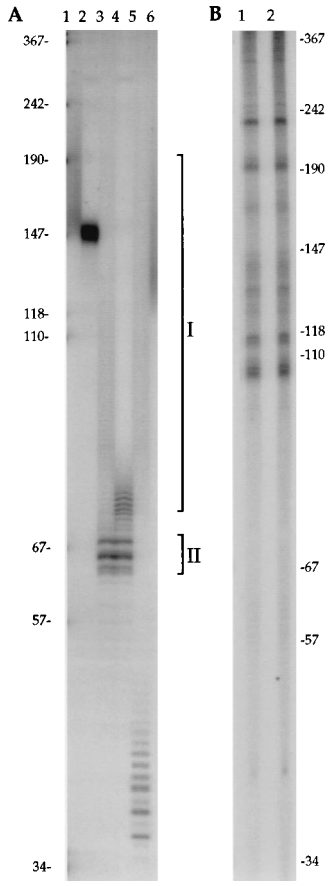

FIG. 6. Identification of polyadenylated plus-strand leader RNAs. Radiolabeled RNA from a 30-min incubation in vitro was fractionated on an oligo(dT)-cellulose column, and aliquots of the bound fraction (A) or the effluent fraction (B) were analyzed by RNase H digestion. RNase H digestions in the absence of a DNA oligonucleotide are illustrated in lanes 1. (A) Digestions after hybridization to specific oligonucleotides are shown in lane 2 [oligo(dT)], lane 3 (L68), lane 4 [L68 plus oligo(dT)], lane 5 (L68 plus L22), and lane 6 (L22). (B) Lane 2 shows digestion after hybridization to L68 plus oligo(dT). The digestion products were resolved on a denaturing 8% polyacrylamide gel. The locations of single-stranded DNA size markers (in nucleotides) are shown on the left side of panel A and the right side of panel B. To the right side of panel A, two RNA clusters discussed in the text are identified. Cluster I is visible in lanes 3 and 5; cluster II is visible in lanes 3 and 4.

detected (Fig. 6A, compare lane 5 with lane 3). This result indicates that cluster II corresponded to the 5′ end of the leader RNA. Digestion of the RNA with L22 alone cleaved the RNAs into a smaller smear, corroborating that the size heterogeneity was due to variation at the 3′ end of the molecules (Fig. 6A, lane 6). Hence, these experiments clearly demonstrated that RNA molecules that correspond to the plus-strand leader RNAs identified in SYNV-infected cells were synthesized in vitro and that these molecules had 3′-terminal poly(A) extensions ranging from 10 to 100 nt. In similar experiments, the RNA that was not retained by the oligo(dT) matrix [poly(A)-minus fraction] was also treated with RNase H in the absence of an oligonucleotide (Fig. 6B, lane 1) or after hybridization to L68 (Fig. 6B, lane 2). Since cluster II was not detected in Fig. 6B, lane 2, the latter result suggested that the vast majority of plus-strand leader RNA synthesized in vitro in the 30-min reaction was both full-length and polyadenylated.

Identification of SYNV proteins in the purified nuclei and polymerase extract. The proteins present in nuclei, in the polymerase and control extracts, and in virus particles were compared by using SDS-PAGE followed by silver staining (Fig. 7A). Inspection of silver-stained samples from infected nuclei and, in particular, polymerase extracts revealed that two of the most intensely stained polypeptides in the preparations comigrated with the SYNV N and M2 proteins present in the virus preparation (Fig. 7A, lanes 1 and 3). These polypeptides were absent from preparations of mock-infected tissue, further suggesting that they were viral proteins (Fig. 7A, lanes 2 and 4). Aside from the viral polypeptides, similar protein profiles were detected by silver staining in the infected versus the mock-infected nuclei (Fig. 7A, lanes 1 and 2) and in the polymerase versus the control nuclear extracts (Fig. 7A, lanes 3 and 4).

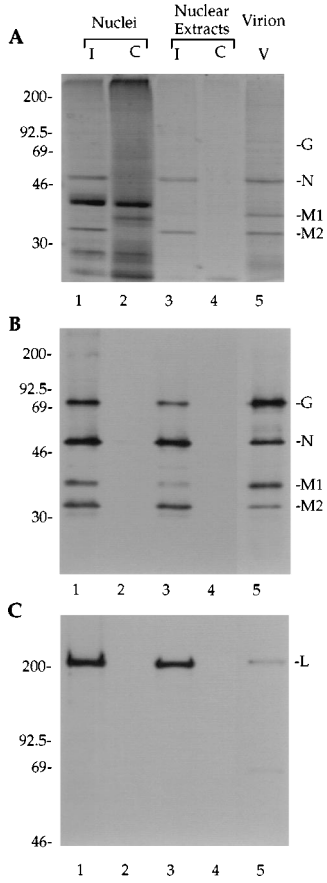

FIG. 7. Analysis of proteins present in purified tobacco leaf nuclei and in nuclear extracts. Shown are protein profiles in nuclei from infected and control plants (lanes 1 and 2), extracts from these nuclei (lanes 3 and 4), and purified virions (lanes 5) after denaturation and separation by SDS–10% (A and B) or –6% (C) PAGE. The locations of the SYNV proteins are shown on the right, and the molecular mass markers (in kilodaltons) are illustrated on the left. (A) Silver staining of a gel containing 1 μg of proteins from the nuclei, 0.2 μg of proteins from the nuclear extracts, or 0.3 μg of proteins from purified virions. Note that the SYNV G protein is negatively stained, as is visible in the virion sample. (B) Immunoblot analysis using SYNV virion-specific antiserum. Hybridization was visualized with alkaline phosphatase-conjugated secondary antibodies and bromochloroindoyl phosphate-nitroblue tetrazolium. Lanes containing the SYNV proteins were loaded such that the N protein concentration in each sample was approximately the same (as determined by comparing a dilution series probed with the SYNV antiserum [data not shown]). The concentration of proteins in the preparations from noninfected tissue (lanes 2 and 4), as determined by silver staining (not shown), was equal to or greater than those in each corresponding sample from infected tissue. (C) L-specific immunoblot analysis. The immunoblot was probed with an antiserum raised against a peptide fusion containing a portion of the SYNV L gene overexpressed in bacteria. Hybridization was visualized with enhanced chemiluminescence (Amersham). Twice the amount of each sample used in panel B was loaded.

The viral proteins in the preparations were investigated further by using rabbit polyclonal antibodies raised against disrupted virions (30) (Fig. 7B) and mouse ascites antibodies elicited by an sc4–glutathione *S*-transferase fusion protein (55) (data not shown) and by a fusion protein containing a portion of the L protein, which was prepared during the course of these experiments (Fig. 7C). The SYNV-specific antiserum (α-SYNV) reacts with at least four proteins: G, N, M1, and M2 (30). As shown in Fig. 7B, all four of these proteins were readily detected in the nuclei and in the polymerase extracts from the SYNV-infected tobacco leaves. The N and M2 proteins comigrated with the two most prominent proteins detected by silver staining in the polymerase extract, confirming that the silver-stained proteins were SYNV N and M2 (compare Fig. 7B and 7A, lanes 1 and 3). Furthermore, comparison of samples from the virion and polymerase extracts (Fig. 7B, lanes 5 and 1) reveals that the relative proportions of the N and M2 proteins, compared with either G (which was not detected by silver staining [Fig. 7A]) or M1, were higher in the polymerase extract than in the purified virions.

The samples were also probed with L-specific ascites fluid (Fig. 7C). This ascites fluid reacted with a single polypeptide present in the virions, the nuclei, and the polymerase extracts from infected cells but failed to react with proteins from noninfected nuclei or from control nuclear extracts. The detected polypeptide migrated slightly more slowly than the 200-kDa marker on the SDS-polyacrylamide gel. The amount of L protein reactivity in the polymerase extract sample exceeded that in the virion sample, suggesting that the relative level of L, compared with G or M1, was also higher in the polymerase extract than in purified virions (Fig. 7C and B). Finally, with an sc4-specific antibody, the sc4 gene product was not detected in the infected nuclei or in polymerase extracts (data not shown).

DISCUSSION

In this communication, we report the partial purification of an SYNV-specific polymerase from infected plant tissue. The RNA products synthesized in vitro included the SYNV plus-strand leader RNA and full-length N and M2 mRNAs (Fig. 5 and 6). Each of these viral RNA products was previously detected in vivo in SYNV-infected plants and protoplasts (33, 51, 62). The activity detected was found exclusively in preparations derived from SYNV-infected leaves (Fig. 2 and 4) and was insensitive to DNase I, which was routinely included in the transcription reactions. Furthermore, significant incorporation of radiolabeled UTP into virus-specific RNA required all four ribonucleotides with an available 3′ hydroxyl group, as expected for an RNA chain elongation reaction (Fig. 4). Taken together, therefore, these results demonstrate that an SYNV-specific RNA-dependent RNA polymerase activity can be extracted from the nuclei of infected tissue by the protocols we have developed.

The data suggest that viral transcription in vitro is biased in a polar or cascade pattern. During the 1-h period assessed here, the most abundant of the SYNV mRNAs synthesized corresponded to the gene located nearest the 3′ end of the genome, the N gene; we detected a lower abundance of full-length products corresponding to the next three genes on the genome, M2, sc4, and M1, whereas full-length mRNA products of the 5′-proximal G and L genes were not detected (Fig. 3). In addition, comparison of the size distribution of products that hybridize to probes for each viral gene (Fig. 3) shows an increase in the proportion of smaller products to full-length RNAs with each successive gene from the N gene (primarily full-length products) to the G and L genes (only smaller products). Overall, therefore, these results are consistent with a cascade pattern in the rate of mRNA accumulation which reflects the location of each gene on the viral genome, from 3′ to 5′. More in-depth analysis of the kinetics of SYNV transcription has substantiated these preliminary observations (60a). A similar cascade transcription pattern, first observed in VSV, is one of the hallmarks of rhabdovirus and paramyxovirus transcription in animals (3, 19, 35). Our results suggest for the first time that this gene expression pattern also may be conserved in the nucleus-localized plant rhabdoviruses.

We provide strong evidence that the plus-strand leader of SYNV is polyadenylated in vitro (Fig. 6). The analysis further suggests that most, if not all, of the leader RNAs synthesized in vitro were polyadenylated at the 3′ end. We were unable to detect any products corresponding to plus-strand leader RNAs in the fraction of RNA that did not bind oligo(dT)-cellulose (Fig. 6B, lane 2), and the majority of those that did bind the matrix appeared to be greater in length than the 147-nt marker (Fig. 6A, lane 2). Digestion with RNase H and oligo(dT) converted the detected leader RNAs into a homogeneous product that was the same size as the genome-encoded portion of the leader RNAs previously detected with RNase protection with an SYNV genomic RNA probe (62). In results very similar to ours, Zuidema et al. have shown previously that all detectable SYNV leader isolated from infected cells is retained on oligo(dT)-cellulose columns (62). Therefore, it is highly likely that a 3′ poly(A) tail is added to the vast majority of SYNV leader RNAs synthesized during viral infection.

Although it is commonly thought that plus-strand leader RNAs of nonsegmented, minus-strand RNA viruses are distinguished from the viral mRNAs by the absence of a poly(A) tail (3), experimental data supporting this generalization are available for only two viruses, VSV and Sendai virus (16, 42). However, examination of the sequence data suggests that plus-strand leader polyadenylation is a feature of SYNV that is not shared by the cytoplasmically replicating nonsegmented minus-strand RNA viruses sequenced to date. Figure 8 shows that three components of the junction sequences between genes of these viruses are generally conserved, a poly(U) tract at the 3′ end of each gene on the genomic template (element I), a short nontranscribed element (II), and a conserved element located at the beginning of the subsequent gene (III) (for a discussion, see references 3 and 35). Comparison of the junction region between the leader and the N gene with the consensus intergenic sequence reveals that SYNV is the only rhabdo- or paramyxovirus sequenced to date in which both elements I and II at the leader-N junction are nearly identical to the consensus gene junction sequence. Both VSV and rabies lack region II at the leader-N junction and, although a short poly(U) sequence is present in region I, the polymerase transverses this region and copies one or more of the subsequent nucleotides (G for VSV, ACA for rabies) during leader synthesis (34, 38). A lettuce necrotic yellows virus (LNYV) plus-strand leader has not been identified to date, so the 3′ end of this molecule is not yet known. Nevertheless, it is clear that the putative regions I and II of the leader-N junction of LNYV are both truncated compared with the consensus sequence separating the mRNAs. In addition, the consensus gene junction sequences and the junction between the leader and the first viral mRNA are shown for four paramyxoviruses (Fig. 8). In these paramyxoviruses, sequences resembling the consensus region II can be identified preceding the first mRNA start site. However, considerable divergence is evident between the conserved element I and the sequence encoding the 3′ ends of the leaders. Elements I and II of the gene junction sequences are believed to have a role in the termination of mRNA synthesis and as a

		I	II	III
SYNV	consensus	**AUUCUUUUU**/	**GG**	/UUG$^{UC}_{AA}$
	leader/N	**AUUUCUUUU**/	**GG**	/UUGUA
VSV	consensus	ACUUUUUUU/	$^{G}_{C}$A	/UUGUC
	leader/N	UCCUCUUUG/	AAA	/UUGUC
Rabies	consensus	ACUUUUUUU/	C(N_n)	/UUGU$^{G}_{A}$
	leader/N	GUUUUU/ACA/	none	/UUGUG
LNYV	consensus	AAUU**CUUUU**	GNUC(N_n)**ACU**	/ACUCU
	leader/N	AGCC**CUUUU**	CUC**ACU**	/ACUCU
Sendai	consensus	UNAUUCUUUUU	**GAA**	/UCCCAN**UUUC**
	leader/N	AAUAUGUCCUA	**AAA**	/UCCCAG**UUUC**
HPIV-3	consensus	[UUUAUUC](U_{5-6})	**GAA**	/UCCUNN**UUUC**
	leader/N	UAAUUUUAAUU	**GAA**	/UCCUAA**UUUC**
Measles	consensus	(U_{4-6})	G^{A}_{C}**A**	/UCCNNNNUNC
	leader/N	UCACGU	**GAA**	/UCCUAAGUUC
RSV	consensus	UCAAU(N_{3-4})(U_4)	not conserved	/CCC$^{C}_{U}$GUUU
	leader/1C	UACCCCGUUUA	n/a	/CCCCGUUU

FIG. 8. Alignment of the leader-N (or leader-1C) junctions and the conserved gene junction sequences of nonsegmented, minus-strand viruses. The consensus gene junction sequences on the genomic RNAs of each virus are presented, including the region encoding the 3′ mRNA end (I), a nontranscribed intergenic region (II), and the 5′ end of the subsequent gene (III). Also shown is the junction between the leader and the first gene on the genomic RNA of each virus. Note that the 3′ end of each sequence is to the left and the 5′ end is to the right. Nucleotides that are conserved between the consensus and the leader junctions in regions I and II are shown in boldface. The sites of termination and initiation of templated transcription are denoted by a slash. HPIV-3, human parainfluenza virus type 3; RSV, respiratory syncytial virus. The 3′ end of the plus-strand leaders of LNYV, Sendai virus, HPIV-3, measles, and respiratory syncytial virus have not been reported, and so the length and identity of a nontranscribed region on the genome preceding the first gene are unknown. Some variation in sequence and location was observed in the HPIV consensus region I in brackets. The sequences are derived as indicated: SYNV (25, 62); VSV (Indiana serotype) (34, 52); rabies virus (38); LNYV (61); and Sendai virus, HPIV-3, measles virus, and respiratory syncytial virus (21, 45).

template for poly(A) tract synthesis through a chattering mechanism involving reiterative transcription of the poly(U) tract (5). Thus, the analysis predicts that the SYNV leader would be polyadenylated, whereas the leader RNAs of the cytoplasmically replicating rhabdoviruses and paramyxoviruses would lack a poly(A) tail. In addition, most of the plus-strand leader templates shown have poly(U) tracts (albeit truncated) near the leader-N junction, and yet SYNV alone has a poly(U) tract directly abutting a conserved region II. This thus suggests that the intergenic region II may be critical for the initiation of polyadenylation process in these viruses.

Why would the SYNV leader be polyadenylated? An interaction between the leader RNA and host poly(A)-specific factors, for instance poly(A)-binding proteins (53), is likely. Such an interaction might have an effect on host gene expression, although if such an effect exists, it is likely transient because comparison of the profiles of radiolabeled proteins synthesized in infected and mock-infected protoplasts by SDS-PAGE has failed to reveal dramatic differences (60a). Alternatively, interactions with host components via the poly(A) tail might affect the subcellular localization of the leader RNA. Polyadenylation of SYNV leader RNA may facilitate the sequestration of these molecules away from the site of transcription and replication via interactions with host components, perhaps through export of the molecules from the nucleus. The nascent VSV leader RNA has been postulated to have an important role in the transition between transcription and replication during infection (6). This RNA is believed to contain the sequences required for encapsidation of the antigenomic RNA by the N protein. Since the availability of N protein that is not incorporated into ribonucleoprotein complexes has been shown to be a critical factor for viral replication (1, 47), it is believed that encapsidation of nascent RNA in the leader region may act as a regulatory switch, causing the polymerase to transverse the intergenic regions during full-length antigenome replication. In vivo experiments with VSV have revealed that the VSV leader RNA is transiently localized in the nucleus early after infection (39). It has been proposed that the VSV leader may inhibit host transcription in the nucleus (44). Another attractive hypothesis, however, is that the transport of these molecules into the nucleus serves to remove them from the site of viral transcription and replication. Removal of the fully synthesized leader RNA from the site of transcription would eliminate competition with the nascent leader RNAs on the transcription complex for available N protein. Nuclear transport of the leader RNA would therefore increase the probability of encapsidation of nascent leader and thereby would facilitate rapid switching from transcription to replication. An important difference between SYNV and VSV is that the SYNV polymerase complex is localized in the nucleus, rather than in the cytoplasm of infected cells; our model suggests that SYNV leader RNA polyadenylation reflects an adaptation to this nuclear localization. The model makes two testable predictions: first, the SYNV leader should be cytoplasmically localized early in infection, or at least localized to a location distinct from the site of transcription in the nucleus; and second, other nonsegmented minus-strand viruses which replicate in the nucleus should synthesize polyadenylated leaders. Both the bornaviruses (54) and a number of plant rhabdoviruses (31) are thought to replicate in cell nuclei. Therefore, it will be interesting to see whether the leaders of these viruses are also polyadenylated.

The present results also provide the first direct evidence that a protein synthesized from the L gene of SYNV is present in both infected cells and virus particles (Fig. 7C). The principal polypeptide detected by Western blotting with antibodies raised against a portion of the L gene migrated slightly more slowly than a 200-kDa marker protein. The size of this polypeptide thus corresponds well with the 241-kDa molecular mass previously deduced from the L-gene primary sequence (11). On the basis of extensive regions of homology between the SYNV L protein and the polymerases of several other unsegmented minus-strand viruses, it has been suggested that the SYNV L protein may be a component of the viral polymerase (11). The relative abundance of this protein in active polymerase preparations is consistent with a polymerase function (Fig. 7).

In conclusion, we report the development of a procedure for partial purification of SYNV polymerase from infected tissue that circumvents the difficulties encountered in using purified virions as a source of viral polymerase. The analysis presented here indicates that the in vitro system retains many of the components of SYNV transcription previously characterized in vivo. Therefore, the system represents a substantial advance in the tools available for the elucidation of SYNV infection.

ACKNOWLEDGMENTS

We thank Caroline Kane, Robert Donald, David Hacker, Diane Lawrence, Tim Petty, Karen-Beth and Herman Scholthof, Doris Wagner, and Huan Zhou for helpful discussions while this work was in progress. We also thank Diane Lawrence, Loy Volkman, and Doris Wagner for critically reading the manuscript.

This research was supported by grants DMB 90-47486 and DMB 94-18086 from the National Science Foundation to A.O.J.

REFERENCES

1. **Arnheiter, H., N. L. Davis, G. Wertz, M. Schubert, and R. A. Lazzarini.** 1985. Role of the nucleocapsid protein in regulating vesicular stomatitis virus RNA synthesis. Cell **41:**259–267.
2. **Baltimore, D., A. S. Huang, and M. Stampfer.** 1970. Ribonucleic acid synthesis of vesicular stomatitis virus, II. An RNA polymerase in the virion. Proc. Natl. Acad. Sci. USA **66:**572–576.
3. **Banerjee, A. K.** 1987. Transcription and replication of rhabdoviruses. Microbiol. Rev. **51:**66–87.
4. **Banerjee, A. K., and S. Barik.** 1992. Gene expression of vesicular stomatitis virus genome RNA. Virology **188:**417–428.
5. **Banerjee, A. K., S. A. Moyer, and D. P. Rhodes.** 1974. Studies on the in vitro adenylation of RNA by vesicular stomatitis virus. Virology **61:**547–558.
6. **Blumberg, B. M., M. Leppert, and D. Kolakofsky.** 1981. Interaction of VSV leader RNA and nucleocapsid protein may control VSV genome replication. Cell **23:**837–845.
7. **Bradford, M. M.** 1976. A rapid and sensitive method for the quantitation of microgram quantities of protein utilizing the principle of protein-dye binding. Anal. Biochem. **72:**248–254.
8. **Bras, F., D. Teninges, and S. Dezelee.** 1994. Sequences of the N and M genes of the sigma virus of Drosophila and evolutionary comparison. Virology **200:** 189–199.
9. **Carlsen, S. R., R. W. Peluso, and S. A. Moyer.** 1985. In vitro replication of Sendai virus wild-type and defective interfering particle genome RNAs. J. Virol. **54:**493–500.
10. **Choi, T.-J.** 1993. Ph.D. thesis. University of California, Berkeley.
11. **Choi, T.-J., S. Kuwata, E. V. Koonin, L. A. Heaton, and A. O. Jackson.** 1992. Structure of the L (polymerase) protein gene of sonchus yellow net virus. Virology **189:**31–39.
12. **Choi, T.-J., J. D. Wagner, and A. O. Jackson.** 1994. Sequence analysis of the trailer region of sonchus yellow net virus genomic RNA. Virology **202:**33–40.
13. **Christie, S. R.** 1969. Nicotiana hybrid developed as a host for plant viruses. Plant Dis. Rep. **53:**939–941.
14. **Christie, S. R., R. G. Christie, and J. R. Edwardson.** 1974. Transmission of a bacilliform virus of sowthistle and *Bidens pilosa*. Phytopathology **64:**840–845.
15. **Citovsky, V., D. Knorr, G. Schuster, and P. Zambryski.** 1990. The P30 movement protein of tobacco mosaic virus is a single-strand nucleic acid binding protein. Cell **60:**637–647.
16. **Colonno, R. J., and A. K. Banerjee.** 1978. Complete nucleotide sequence of the leader RNA synthesized in vitro by vesicular stomatitis virus. Cell **15:**93–101.
17. **Dignam, J. D., R. M. Lebovitz, and R. G. Roeder.** 1983. Accurate transcription initiation by RNA polymerase II in a soluble extract from isolated mammalian nuclei. Nucleic Acids Res. **11:**1475–1489.
18. **Dolja, V. V., H. J. McBride, and J. C. Carrington.** 1992. Tagging of plant potyvirus replication and movement by insertion of beta-glucuronidase into the viral polyprotein. Proc. Natl. Acad. Sci. USA **89:**10208–10212.
19. **Emerson, S. U.** 1987. Transcription of vesicular stomatitis virus, p. 245–270. *In* R. R. Wagner (ed.), The rhabdoviruses. Plenum Press, New York.
20. **Flore, P. H.** 1986. Ph.D. thesis. Landbouwhogeschool te Wageningen, Wageningen, The Netherlands.
21. **Galinski, M. S.** 1991. Annotated nucleotide and protein sequences for selected *Paramyxoviridae*, p. 537–568. *In* D. W. Kingsbury (ed.), The paramyxoviruses. Plenum Press, New York.
22. **Goldberg, K. B., B. Modrell, B. I. Hillman, L. A. Heaton, T.-J. Choi, and A. O. Jackson.** 1991. Structure of the glycoprotein gene of sonchus yellow net virus, a plant rhabdovirus. Virology **185:**32–38.
23. **Harlow, E., and D. Lane.** 1988. Antibodies: a laboratory manual. Cold Spring Harbor Laboratory Press, Cold Spring Harbor, N.Y.
24. **Hearne, P. Q., D. A. Knorr, B. I. Hillman, and T. J. Morris.** 1990. The complete genome structure and synthesis of infectious RNA from clones of tomato bushy stunt virus. Virology **177:**141–151.
25. **Heaton, L. A., B. I. Hillman, B. G. Hunter, D. Zuidema, and A. O. Jackson.** 1989. Physical map of the genome of sonchus yellow net virus, a plant rhabdovirus with six genes and conserved gene junction sequences. Proc. Natl. Acad. Sci. USA **86:**8665–8668.
26. **Heaton, L. A., D. Zuidema, and A. O. Jackson.** 1987. Structure of the M2 protein gene of sonchus yellow net virus. Virology **161:**234–241.
27. **Heintz, N., and R. G. Roeder.** 1984. Transcription of human histone genes in extracts from synchronized HeLa cells. Proc. Natl. Acad. Sci. USA **81:**2713–2717.
28. **Hill, V. M., and D. F. Summers.** 1982. Synthesis of VSV RNPs in vitro by cellular VSV RNPs added to uninfected HeLa cell extracts: VSV protein requirements for replication in vitro. Virology **123:**407–419.
29. **Hillman, B. I., L. A. Heaton, B. G. Hunter, B. Modrell, and A. O. Jackson.** 1990. Structure of the gene encoding the M1 protein of sonchus yellow net virus. Virology **179:**201–207.
30. **Jackson, A. O.** 1978. Partial characterization of the structural proteins of sonchus yellow net virus. Virology **87:**172–181.
31. **Jackson, A. O.** 1987. Biology, structure, and replication of plant rhabdoviruses, p. 427–508. *In* R. R. Wagner (ed.), The rhabdoviruses. Plenum Press, New York.
32. **Jackson, A. O., and S. R. Christie.** 1977. Purification and some physiochemical properties of sonchus yellow net virus. Virology **77:**344–355.
33. **Jones, R. W., and A. O. Jackson.** 1990. Replication of sonchus yellow net virus in infected protoplasts. Virology **179:**815–820.
34. **Keene, J. D., M. Schubert, and R. A. Lazzarini.** 1980. Intervening sequence between the leader region and the nucleocapsid gene of vesicular stomatitis virus RNA. J. Virol. **33:**789–794.
35. **Kingsbury, D. W.** 1990. Paramyxoviridae and their replication, p. 945–962. *In* B. N. Fields and D. M. Knipe (ed.), Virology, 2nd ed., vol. 1. Raven Press, New York.
36. **Konforti, B. B., M. J. Koziolkiewicz, and M. M. Konarska.** 1993. Disruption of base pairing between the 5′ splice site and the 5′ end of U1 snRNA is required for spliceosome assembly. Cell **75:**863–873.
37. **Krämer, A., and W. Keller.** 1990. Preparation and fractionation of mammalian extracts active in pre-mRNA splicing. Methods Enzymol. **181:**3–19.
38. **Kurilla, M. G., C. D. Cabradilla, B. P. Holloway, and J. D. Keene.** 1984. Nucleotide sequence and host La protein interactions of rabies virus leader RNA. J. Virol. **50:**773–778.
39. **Kurilla, M. G., H. Piwnica-Worms, and J. D. Keene.** 1982. Rapid and transient localization of the leader RNA of vesicular stomatitis virus in the nuclei of infected cells. Proc. Natl. Acad. Sci. USA **79:**5240–5244.
40. **Lamb, R. A., and P. W. Choppin.** 1983. The gene structure and replication of influenza virus. Annu. Rev. Biochem. **52:**467–506.
41. **Leppert, M., and D. Kolakofsky.** 1978. 5′ terminus of defective and nondefective Sendai virus genomes is ppp Ap. J. Virol. **25:**427–432.
42. **Leppert, M., L. Rittenhouse, J. Perrault, D. F. Summers, and D. Kolakofsky.** 1979. Plus and minus strand leader RNAs in negative strand virus-infected cells. Cell **18:**735–747.
43. **Luthe, D. S., and R. S. Quatrano.** 1980. Transcription in isolated nuclei. II. Characterization of RNA synthesized *in vitro*. Plant Physiol. **65:**309–313.
44. **McGowan, J. J., S. U. Emerson, and R. R. Wagner.** 1982. The plus-strand leader RNA of VSV inhibits DNA-dependent transcription of adenovirus and SV40 genes in a soluble whole-cell extract. Cell **28:**325–333.
45. **Mink, M. A., D. S. Stec, and P. L. Collins.** 1991. Nucleotide sequences of the 3′ leader and 5′ trailer regions of human respiratory syncytial virus genomic RNA. Virology **185:**615–624.
46. **Moore, C. L.** 1990. Preparation of mammalian extracts active in polyadenylation. Methods Enzymol. **181:**49–74.
47. **Patton, J. T., N. L. Davis, and G. W. Wertz.** 1984. N protein alone satisfies the requirement for protein synthesis during RNA replication of vesicular stomatitis virus. J. Virol. **49:**303–309.
48. **Petty, I. T., B. G. Hunter, and A. O. Jackson.** 1988. A novel strategy for one-step cloning of full-length cDNA and its application to the genome of barley stripe mosaic virus. Gene **74:**423–432.
49. **Poch, O., B. M. Blumberg, L. Bougueleret, and N. Tordo.** 1990. Sequence comparison of five polymerases (L proteins) of unsegmented negative-strand RNA viruses: theoretical assignment of functional domains. J. Gen. Virol. **71:**1153–1162.
50. **Restrepo, M. A., D. D. Freed, and J. C. Carrington.** 1990. Nuclear transport of plant potyviral proteins. Plant Cell **2:**987–998.
51. **Rezaian, M. A., L. A. Heaton, K. Pederson, J. J. Milner, and A. O. Jackson.** 1983. Size and complexity of polyadenylated RNAs induced in tobacco infected with sonchus yellow net virus. Virology **131:**221–229.
52. **Rose, J. K.** 1980. Complete intergenic and flanking gene sequences from the genome of vesicular stomatitis virus. Cell **19:**415–421.
53. **Sachs, A., and E. Wahle.** 1993. Poly(A) tail metabolism and function in eucaryotes. J. Biol. Chem. **268:**22955–22958.
54. **Schneemann, A., P. A. Schneider, R. A. Lamb, and W. I. Lipkin.** 1995. The remarkable coding strategy of Borna disease virus: a new member of the nonsegmented negative strand RNA viruses. Virology **210:**1–8.
55. **Scholthof, K. B., B. I. Hillman, B. Modrell, L. A. Heaton, and A. O. Jackson.** 1994. Characterization and detection of sc4: a sixth gene encoded by sonchus yellow net virus. Virology **204:**279–288.
56. **Schumacher, J., H. L. Sänger, and D. Riesner.** 1983. Subcellular localization of viroids in highly purified nuclei from tomato leaf tissue. EMBO J. **2:**1549–1555.
57. **Studier, F. W., A. H. Rosenberg, J. J. Dunn, and J. W. Dubendorff.** 1990. Use of T7 RNA polymerase to direct expression of cloned genes. Methods Enzymol. **185:**60–89.
58. **Towbin, H., T. Staehelin, and J. Gordon.** 1979. Electrophoretic transfer of proteins from polyacrylamide gels to nitrocellulose sheets: procedure and some applications. Proc. Natl. Acad. Sci. USA **76:**4350–4354.
59. **van Beek, N. A. M., D. Lohuis, J. Dijkstra, and D. Peters.** 1985. Morphogenesis of sonchus yellow net virus in cowpea protoplasts. J. Ultrastruct. Res. **90:**294–303.
60. **Wagner, J. D. O.** 1995. Ph.D. thesis. University of California, Berkeley.

60a. **Wagner, J. D. O., and A. O. Jackson.** Unpublished data.

61. **Wetzel, T., R. G. Dietzgen, and J. L. Dale.** 1994. Genomic organization of lettuce necrotic yellows rhabdovirus. Virology **200:**401–412.
62. **Zuidema, D., L. A. Heaton, R. Hanau, and A. O. Jackson.** 1986. Detection and sequence of plus-strand leader RNA of sonchus yellow net virus, a plant rhabdovirus. Proc. Natl. Acad. Sci. USA **83:**5019–5023.
63. **Zuidema, D., L. A. Heaton, and A. O. Jackson.** 1987. Structure of the nucleocapsid protein gene of sonchus yellow net virus. Virology **159:**373–380.